Temperature-dependent NMR study of the impurity state in heavily doped Si:P

Ernesta M. Meintjes,* Jeremy Danielson, and William W. Warren, Jr.
Department of Physics, Oregon State University, Corvallis, Oregon 97331-6501, USA
(Received 21 May 2004; revised manuscript received 5 October 2004; published 26 January 2005)

We report ^{31}P (impurity) and ^{29}Si (host) nuclear magnetic resonance (NMR) data for heavily doped Si:P over a wide temperature range (100–500 K) for samples with nominal doping levels between 4×10^{18} cm^{-3} and 8×10^{19} cm^{-3}. The data include resonance shifts, linewidths, and spin-lattice relaxation rates for both host and impurity nuclei. The NMR parameters for ^{31}P exhibit complex dependences on temperature and dopant concentration that are distinct from those of the host ^{29}Si nuclei indicating that the hyperfine fields at the impurity are determined by local characteristics of the impurity electronic state. For nominal carrier concentrations up to about 1×10^{19} cm^{-3}, the impurity NMR properties are inconsistent with expectation for fully ionized dopants with carriers exclusively occupying states in the conduction band. A simple impurity band model yields numerical simulations of the resonance shifts and relaxation rates that reproduce the qualitative features and are in semi-quantitative agreement with the ^{31}P data. These results imply that free carriers in Si:P are in dynamic exchange with residual impurity states at concentrations as high as 10^{19} cm^{-3} and at temperatures well above room temperature.

DOI: 10.1103/PhysRevB.71.035114 PACS number(s): 71.55.Cn, 76.60.Cq, 76.60.Es

I. INTRODUCTION

The microscopic electronic structure of donor and acceptor impurities in silicon represents one of the most thoroughly investigated subjects in condensed matter physics. The reasons are quite clear. Intelligent use of dopants is critical in determining the specific electronic properties necessary for the many applications of silicon technology. Furthermore, because the electronic character of doped silicon ranges from highly insulating to metallic as the dopant concentration is varied, doped silicon has become a "fruit fly" system for the basic investigation of the metal-nonmetal (MNM) transition. Doped silicon may well be the best characterized material in existence for such studies. Very recently, doped silicon has attracted additional interest as a candidate material for quantum computing applications.

The electronic structure of isolated donors and acceptors in lightly doped material has been understood in some detail for decades.[1] At concentrations near and above that of the MNM transition, however, interplay of strong impurity-impurity interactions with the inherent disorder of a doped material leads to a more complex situation. This regime remains incompletely understood despite considerable effort, much of which has been focused on the ground-state electronic properties at very low temperatures. For example, a classic investigation of the dc electrical conductivity through the MNM transition extended into the mK temperature range.[2] Such studies and extensive work on low-temperature magnetic properties[3–12] of doped silicon lead to a picture of a highly inhomogeneous local electronic structure in which, even well above the MNM transition, electrons localized on impurity sites coexist with mobile electrons in delocalized states.

Despite progress achieved at very low temperatures, there is additional insight to be gained from investigation of electronic properties under conditions of thermal excitation. One of the outstanding problems concerns broadening into impurity bands of the electronic ground and low-lying excited states of isolated dopants, and the eventual fate of these impurity bands at ever higher dopant concentrations. Physical properties depend on the thermal distribution of electron occupation over the impurity levels. Consequently, measurements taken over ranges of temperature comparable with the impurity bandwidths and binding energies should reveal the existence and fundamental features of the impurity electronic structure. Studies of the temperature-dependent optical properties of Si:P, for example, have yielded clear evidence of structured impurity bands in the concentration range between the MNM transition ($\sim4\times10^{18}$ cm^{-3}) and 1×10^{19} cm^{-3}.[13] The optical experiments show evidence of the shift of population from the lowest impurity states to the conduction band as the temperature is raised toward room temperature. Of particular interest in all such studies is the role of impurity bands in determining the electronic properties near room temperature at which most applications of doped silicon occur.

Nuclear magnetic resonance (NMR) is a highly local, atomic-scale probe that has been used extensively for study of heavily doped silicon.[3,6–11,14] NMR is well-suited to this problem because the NMR parameters (resonance frequencies, linewidths, and spin-lattice relaxation times) are determined primarily by magnetic hyperfine interactions between the resonant nuclei and unpaired electrons associated with the dopants. Most of these experiments made use of the ^{29}Si host NMR signals and much of the work was done at temperatures of 4.2 K and below. NMR studies using dopant nuclei such as ^{31}P or ^{11}B are, in principle, much more sensitive to the local impurity electronic structure but are inherently difficult because of the weak signals obtained from low concentrations of these species. Nevertheless, the literature contains several reports[3,6,8,10] of ^{31}P and ^{11}B NMR in silicon in which the sensitivity advantage of helium temperature measurement was exploited. As we discuss in more detail elsewhere in this paper, some of these experiments were instrumental in establishing the "two component" model in which localized and itinerant electrons coexist at low temperatures over a range of concentrations above the MNM transition.

The earlier impurity NMR studies in silicon were carried out using magnetic fields that were relatively low (<2 T)) by contemporary standards. In the present work, we have taken advantage of improved sensitivity for ^{31}P in an 8 T magnetic field to probe the local electronic properties of P donors in silicon in the range of nominal concentrations between 4×10^{18} cm^{-3} and 8×10^{19} cm^{-3}, and at temperatures mainly between 100 and 500 K. For purposes of comparison with the impurity NMR properties, we also present complementary results for the resonance shifts, linewidths, and spin-lattice relaxation rate of the host ^{29}Si nuclei in our samples. The present ^{31}P experiments represent an extension of our earlier temperature-dependent ^{11}B NMR studies of the B acceptor in silicon.[15] The somewhat unexpected results of those experiments first suggested to us the possibility of using NMR measurements over a wide temperature range as a probe of electronic structure associated with the dopant.

From measurements of the ^{31}P resonance shifts and spin-lattice relaxation rates, we find that the local magnetic environments of the donors are dominated by electronic states associated with the impurity. Thermal excitation effects dramatically affect the local magnetic properties, but the impurity states continue to play an important role well above room temperature and at nominal phosphorous concentrations up to 10^{19} cm^{-3}. We will show that the basic features of the data can be reproduced with a homogeneous impurity band model that represents the average effects of the inhomogeneous electronic structure detected in the low-temperature experiments. Residual occupation of states in these bands implies that electronic transport at room temperature cannot be described simply in terms of free carriers in the conduction band. Rather, our interpretation suggests that a dynamic equilibrium exists between bands of states derived from the electronic states of the impurities and the conduction states associated with the host crystal.

II. EXPERIMENTAL METHODS

Most of the samples used for these experiments were prepared from wafers obtained from a commercial source.[16] To assure radio-frequency penetration for NMR studies, a portion of each wafer was powdered by crushing in an agate mortar. The nominal room temperature carrier concentrations determined by dc resistivity for four of these samples ranged from 2×10^{18} to 1×10^{19} cm^{-3}. A fifth powder sample with nominal carrier concentration of 8×10^{19} cm^{-3} provided by Holcomb had been used in previous NMR studies of heavily doped silicon.[6] The designations and characteristics of the individual samples are summarized in Table I.

The NMR experiments were carried out using a Varian/Chemagnetics CMX-340 spectrometer operating with a magnetic field of 8.0 T. The resonance lines of ^{29}Si were obtained by Fourier transformation of the free induction decay. For the broader lines exhibited by ^{31}P, it was necessary to record the frequency dependence of the integrated spin echo intensity by stepping through the resonance "point by point." The echoes were obtained with a conventional Hahn sequence of approximately 90°–180° pulse sequences. The pulse separation in the spin-echo sequence was 50 μs. To achieve adequate signal-to-noise ratios for ^{31}P, approximately 100 000 signals were typically recorded and averaged. Resonance shifts for ^{29}Si were measured with respect to a sample of 6N pure silicon powder; for ^{31}P, the shift reference was dilute H_3PO_4. Spin-lattice relaxation times were measured by the saturation-recovery method for ^{29}Si and by the inversion-recovery method for ^{31}P.

TABLE I. Resistivity and nominal carrier concentrations of Si:P samples at 300 K.

Sample designation	Resistivity (Ω cm)	Nominal concentration (cm^{-3})
2	0.0157 ± 0.0016	2×10^{18}
4	0.0115 ± 0.0003	4×10^{18}
7	0.0069 ± 0.0004	7×10^{18}
10	0.0050 ± 0.0007	1×10^{19}
80		8×10^{19}

Variable sample temperatures below room temperature were obtained using flowing, cooled air, or nitrogen. Flowing, heated air was used for measurements above room temperature. In one case (sample 10), measurements were made at 77 K with the sample immersed in liquid nitrogen. A platinum resistance thermometer was used to determine the sample temperatures.

Samples 4, 7, and 10 were further characterized by van der Pauw Hall effect measurements.[17] Squares of approximately 1 cm^2 were cut from the original wafers. Leads attached to the four corners with indium solder were checked for ohmic contact behavior. The measurements were carried out at fields up to 2.6 T. Voltages were measured with field reversal and the results for the two field directions were averaged. Hall coefficients and resistivities were measured at room temperature and at 77 K with the samples immersed in liquid nitrogen

III. EXPERIMENTAL RESULTS

A. ^{31}P impurity NMR

1. Spin echo spectra

An example of temperature-dependent ^{31}P spin echo spectra is shown in Fig. 1 for our sample (7) with nominal carrier concentration $n=7\times10^{18}$ cm^{-3}. The measurements cover the range 77–468 K. Data for the other concentrations are qualitatively similar although the minimum temperature investigated for those samples was approximately 100 K. These measurements show a progressive shift of the resonance peak to higher frequency as the temperature is reduced. Although the linewidths gradually increase with decreasing temperature, the resonance shifts are essentially homogeneous in that for a given change of temperature, the change of shift exceeds the increase in linewidth. That is, to a good approximation the *entire distribution* of local fields shifts to higher values as the temperature decreases. We note that the present observations differ qualitatively from the ^{31}P impurity NMR data previously obtained at 4.2 K and below.[3,6,8,10] In

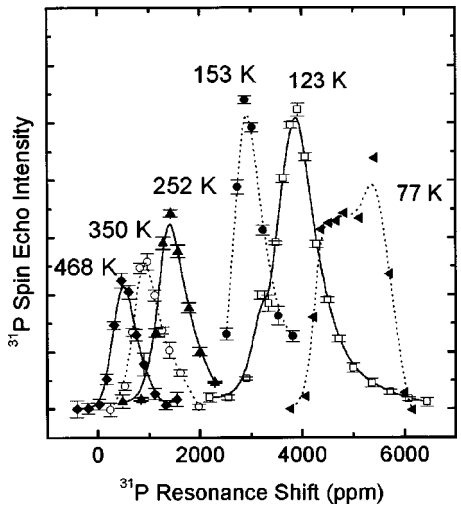

FIG. 1. ^{31}P spin-echo spectra at various temperatures for sample 7 with nominal concentration $n=7\times10^{18}$ cm^{-3}.

samples of comparable doping concentrations at those low temperatures, inhomogeneously broadened spectra extend over a range of frequencies more than an order of magnitude greater than we observe above 77 K. Furthermore, in contrast with the present results, the average resonance shifts were essentially independent of temperature below 4.2 K.

The ^{31}P spin-echo spectra linewidths (full width at half maximum) for all samples are plotted versus temperature in Fig. 2. The linewidths at a given temperature increase monotonically with increasing carrier concentration and the linewidths of all samples increase with decreasing temperature. Samples 7 and 10 are particularly interesting in that they exhibit a sharp onset of increased broadening below about 100 and 150 K, respectively.

^{31}P resonance shifts for all samples are shown as functions of temperature in Fig. 3. In most cases, these shifts correspond to the frequencies of the peaks of spin-echo spectra such as those shown in Fig. 1. However, in the case of

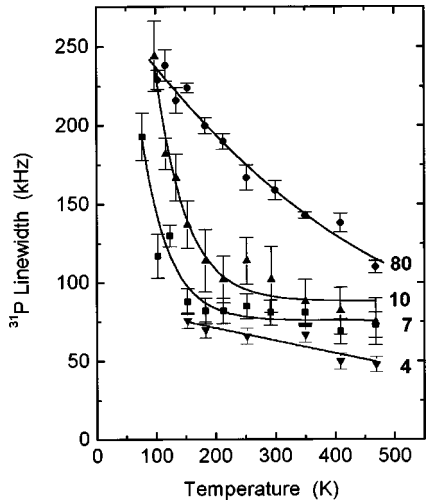

FIG. 2. ^{31}P linewidths (full width at half maximum) versus temperature for samples of different nominal carrier concentrations (in 10^{18} cm^{-3}).

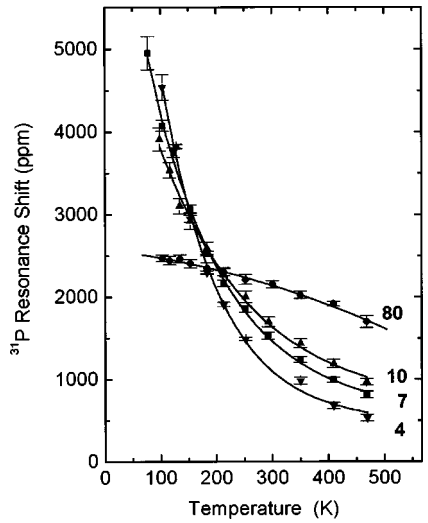

FIG. 3. ^{31}P resonance shifts versus temperature for samples of various nominal carrier concentration (in 10^{18} cm^{-3}).

sample 7 at 77 K, the line shape is rather irregular and we have assigned the shift to the "center-of-gravity" of the line. As noted above, the resonance line for all samples shifts to higher frequency with decreasing temperature. This behavior extends over the full temperature range investigated, with progressively stronger temperature dependence being exhibited with decreasing nominal carrier concentration.

2. Spin-lattice relaxation

The recovery of the ^{31}P nuclear magnetization following an inverting pulse could be fit to single-exponential functions within the precision of the data. The spin-lattice relaxation rates $1/T_1$ thus obtained are shown as a function of temperature in Fig. 4. The temperature dependence of the relaxation rate is qualitatively different for each sample in the range $4-80\times10^{18}$ cm^{-3}. For the highest concentration sample, the rate increases linearly with temperature, behavior typical of a degenerate metal. With decreasing concentration, the temperature dependence progressively decreases, changes sign and, for the lowest concentration, the rate decreases strongly

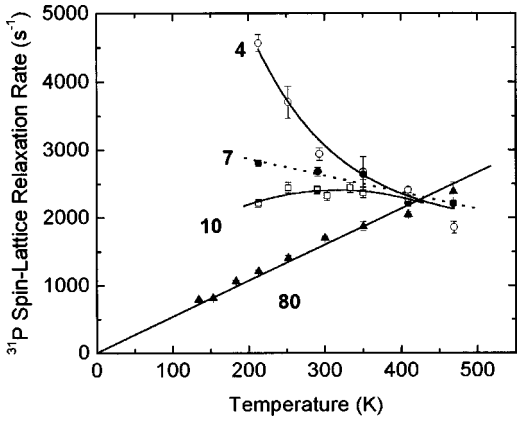

FIG. 4. ^{31}P spin-lattice relaxation rates versus temperature for samples of various nominal carrier concentration (in 10^{18} cm^{-3}).

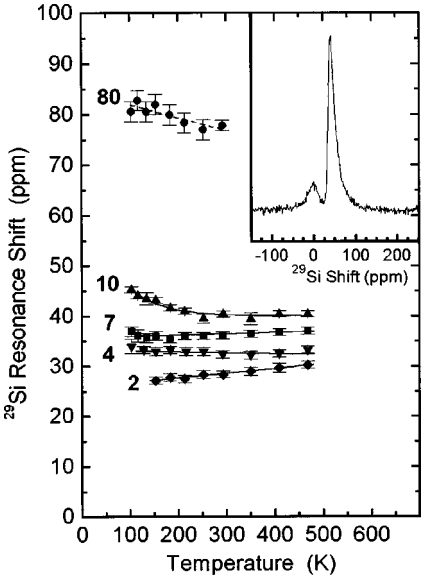

FIG. 5. ^{29}Si resonance shifts versus temperature for samples of various nominal carrier concentration (in 10^{18} cm^{-3}). Inset: representative ^{29}Si spectrum (sample 10 at 292 K). The weak line at approximately zero shift is due to ^{29}Si in the glass ampoule containing the sample.

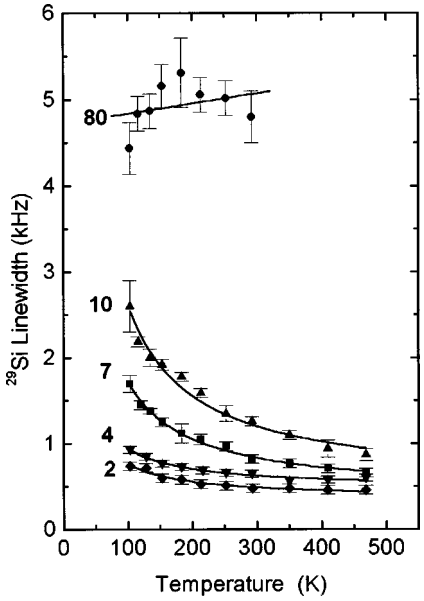

FIG. 6. ^{29}Si linewidths (full width at half maximum) for samples of various nominal carrier concentration (in 10^{18} cm^{-3}).

with temperature. Except for the highest concentration sample (80), low signal-to-noise ratios and the correspondingly long acquisition times limited T_1 measurements to temperatures above 200 K.

B. ^{29}Si Host NMR

1. Resonance shifts and linewidths

The ^{29}Si host resonance shifts are shown as a function of temperature in Fig. 5 for sample concentrations ranging from $2-80\times10^{18}$ cm^{-3}. Also shown in Fig. 5 (inset) is an example of a ^{29}Si spectrum for sample 10 at 292 K. The slight asymmetry shown in this example is typical of the ^{29}Si lines observed in our samples. The ^{29}Si resonance shifts increase monotonically with increasing concentration at all temperatures investigated. For sample 2, the temperature dependence of the shift is positive while, in the more concentrated samples, the shifts are nearly independent of temperature or tend to decrease slightly with increasing temperature.

Linewidths for the ^{29}Si resonances are shown as a function of temperature in Fig. 6. Except for the most highly concentrated sample (80), the linewidths increase significantly with decreasing temperature. Measurements of the integrated intensity of the ^{29}Si resonances indicated progressive loss of signal intensity with decreasing temperature below about 200 K.

2. Spin-lattice relaxation

Spin-lattice relaxation rates $1/T_1$ for ^{29}Si are shown in Fig. 7 as functions of temperature. For $n=80\times10^{18}$ cm^{-3}, the relaxation rate increases linearly with temperature, as was also observed for the ^{31}P relaxation rate in this sample. For the other samples, the temperature dependence is nonlinear and $1/T_1$ varies approximately as $T^{1.6}$.[18] At any temperature, the relaxation rate increases with the concentration. Within the respective experimental errors, these data agree with those of Sundfors and Holcomb[3] for samples of comparable compositions at 300 K. The temperature dependences of the relaxation rates observed in the present experiments are generally consistent with values of $1/T_1$ reported by Sundfors and Holcomb at 77 K.

C. Hall coefficients

The results of Hall effect measurements are summarized in Table II. These measurements were carried out on samples 4, 7, and 10.

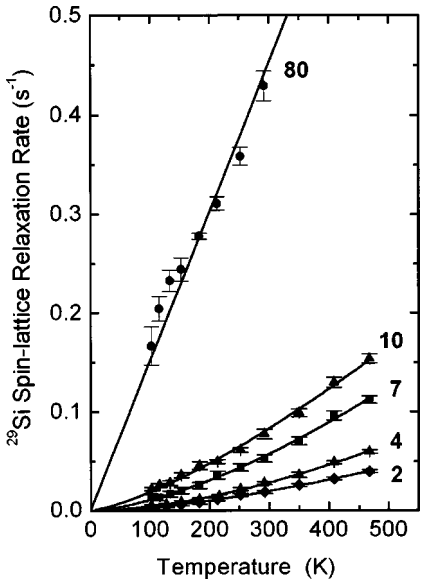

FIG. 7. ^{29}Si spin-lattice relaxation rates versus temperature for samples of various nominal carrier concentration (in 10^{18} cm^{03}).

TABLE II. Values of carrier concentration n_H and mobility μ_H obtained from van der Pauw Hall effect measurements at 77 and 300 K.

Sample (nom. conc.)	$n_H(77)$ (10^{18} cm^{-3})	$n_H(300)$ (10^{18} cm^{-3})	$\mu_H(77)$ (cm^2/V s)	$\mu_H(300)$ (cm^2/V s)
4×10^{18} cm^{-3}	6.8	3.9	61	150
7×10^{18} cm^{-3}	13.0	8.8	99	107
1×10^{19} cm^{-3}	23.4	14.1	98	97

The room-temperature resistivities and Hall coefficients agree within about 20% with literature values for samples with comparable nominal doping levels.[19,20] The decreases in μ_H between room temperature and 77 K are similar to the earlier observations. For example, values of μ_H of 120 and 81 cm^2/V s were reported in Ref. 19 at 300 and 78 K, respectively, for a sample with a room temperature carrier concentration of 5.5×10^{18} cm^{-3}, i.e., intermediate between our samples 4 and 7. As a consequence, the apparent carrier concentrations tend to increase on cooling while the mobility either decreases (lower concentration samples) or remains roughly constant.

IV. INTERPRETATION AND DISCUSSION

A. General observations

An obvious feature of the data obtained in these experiments is the striking difference between the temperature dependences of the NMR properties of ^{31}P and ^{29}Si. Both are sensitive to the dopant concentration, indicating the importance of hyperfine interactions with the spins of extrinsic electrons. But it is evident that the local electronic susceptibility in the vicinity of the phosphorous donors has features that are quite distinct from that probed by the host ^{29}Si nuclei. For example, the ^{31}P resonance shifts of most samples decrease strongly with increasing temperature while those of ^{29}Si are nearly independent of temperature. Similarly, whereas the ^{29}Si relaxation rates increase with temperature for all samples, the ^{31}P rates for the more lightly doped samples decrease with temperature. The exception to this pattern is the very heavily doped sample (80) for which the shifts and relaxation rates of ^{29}Si and ^{31}P are qualitatively similar. We will show that the results for this sample are consistent with expectations for nearly degenerate free carriers confined to the conduction band. In contrast, for samples in the "just metallic" range not too far above the MNM transition (4×10^{18} cm^{-3}–1×10^{19} cm^{-3}), the ^{29}Si and ^{31}P NMR properties imply the existence of a more complex and nonuniform electronic structure. This electronic structure affects the electrical and magnetic properties over wide ranges of temperature.

With regard to the spatial characteristics of the ^{29}Si and ^{31}P NMR properties, it is important to recognize that ^{31}P probes the local environments of the donors while the ^{29}Si NMR properties represent superpositions of the environments of host nuclei having greatly differing separations from the phosphorous dopants. Over the temperature range 100–500 K investigated in the present experiments, the local environments of the ^{31}P nuclei appear to be relatively homogeneous. This is illustrated by spectra such as those shown in Fig. 1 for the sample with $n=7\times10^{18}$ cm^{-3}. Over a given temperature interval, the local magnetic fields experienced by all the observed nuclei change by essentially the same amount. This behavior contrasts sharply with the observations at very low temperatures on samples of comparable doping levels.[3,6,8,10] For example, in the experiments of Alloul and Dellouve,[10] extremely broad spectra were observed, with little or no change of resonance shifts over the range 1.65–4.2 K. Because the magnetic susceptibility of their samples exhibited strong, Curie-like temperature dependence in this range, Alloul and Dellouve concluded that a subset of locally metallic sites were observed in their experiment, while unobserved sites carrying localized spins dominate the susceptibility. The low-temperature results emphasize the essential inhomogeneity of Si(P) associated with the random distribution of dopant atoms in the host crystal. This inhomogeneity is sufficient to produce a "two component" state in which localized spins on some sites coexist with delocalized "metallic" electrons on others. In the temperature range studied in the present experiments, inhomogeneity is expressed by progressive broadening of the ^{31}P resonance with decreasing temperature and the concomitant broadening and loss of intensity of the ^{29}Si resonance.

We argue below that the local magnetic properties of samples with nominal dopant concentrations in the "just metallic" range can be modeled by assuming that the electronic energy levels of the isolated donor survive as a complex of impurity bands. At the temperatures of our experiments, even the qualitative features of the data cannot be understood in terms of conduction band states alone. At 100 K, the local environments of the ^{31}P nuclei are dominated by hyperfine interactions with electrons in the impurity bands. With increasing temperature, the impurity bands are progressively depopulated and thermal broadening suppresses the effects of local variations in the impurity band density of states. These effects lead to strong temperature dependences and apparent homogeneity in the ^{31}P NMR properties at higher temperatures. The picture we present is in overall agreement with inferences from optical data made by Gaymann *et al.*[13] although their work suggests that the impurity bands are essentially depleted by thermal excitation at room temperature. Our data indicate that the average effect of impurity bands influences the local magnetic properties well above room temperature at dopant concentrations as high as 10^{19} cm^{-3}.[21]

B. High concentration limit: $n=8\times10^{19}$ cm^{-3}

We consider first the experimental results for the most heavily doped sample (80) which establish a benchmark at the "metallic" end of our concentration range. A simple test for the NMR properties of a simple, degenerate metal is provided by the Korringa relation[22] between the resonance shift and the spin-lattice relaxation time

$$\left(\frac{\Delta\nu}{\nu}\right)^2 T_1T=\frac{\hbar}{4\pi k_B}\left(\frac{\gamma_e}{\gamma_n}\right)^2, \tag{1}$$

where γ_e and γ_n are, respectively, the electronic and nuclear gyromagnetic ratios and k_B is the Boltzmann constant. For

^{31}P, the Korringa product $(\Delta\nu/\nu)^2 T_1 T$ has the theoretical value 1.603×10^{-6} s K; the experimental value for sample 80 at 300 K is 0.83×10^{-6} s K. For ^{29}Si, the theoretical Korringa product is 6.66×10^{-6} s K which can be compared with the experimental value 4.0×10^{-6} s K. Thus, the shifts and relaxation rates of both species in this sample agree with the Korringa relation to within a factor of 2. Moreover, the relaxation rates $1/T_1$ (Figs. 4 and 7) are nearly linear in temperature, and the shifts (Figs. 3 and 5) are weakly dependent on temperature. These are the expectations for a simple metal.

The Korringa relation is applicable to a degenerate metal, i.e., a case in which the Fermi energy $E_F \gg k_B T$. For $n=8\times10^{19}$ cm^{-3}, the Fermi temperature $T_F=E_F/k_B=730$ K so that over most of the temperature range of our experiments, the electron statistics are only "nearly degenerate." This situation can be addressed through the use of expansions in T/T_F along the lines of the well-known Sommerfeld expansion.[23] Hoch and Holcomb have taken this approach to obtain the leading-term corrections to the Korringa relation for the regimes $T<T_F$ and $T>T_F$ and have applied these relations to an interpretation of our data.[24] However, because we encounter conditions with $T\cong T_F$ for samples with lower dopant concentrations, we employ the exact results which can be evaluated by numerical integration.

The result for the resonance shift is

$$\frac{\Delta\nu}{\nu}=\frac{8\pi}{3}\langle|\phi(0)|^2\rangle\Omega\frac{\mu_B^2}{k_BT}\int_{-\infty}^{\infty}N(E)f(E)[1-f(E)]dE, \quad (2)$$

where μ_B is the Bohr magneton, $N(E)$ is the density of states per unit volume (for both directions of spin), and Ω is the atomic volume of the resonant species. The Fermi distribution function is

$$f(E)=\frac{1}{\exp[(E-\mu)/k_BT]+1} \quad (3)$$

in which μ is the chemical potential $[\mu(T=0)=E_F]$. The chemical potential is fixed at a given temperature by the condition

$$\int_{-\infty}^{\infty}N(E)f(E)dE=n. \quad (4)$$

Including the effect of the six-fold degeneracy at the band minimum of Si, the conduction band density of states is given by

$$N(E)=\frac{6}{2\pi^2}\left(\frac{2m_{\rm eff}}{\hbar^2}\right)^{3/2}E^{1/2} \quad (5)$$

with $m_{\rm eff}=0.33m_0$. A similar relation gives the spin-lattice relaxation rate

$$\frac{1}{T_1}=\frac{16\pi^3}{9}\hbar^3\gamma_e^2\gamma_n^2\langle|\phi(0)|^4\rangle\Omega^2\int_{-\infty}^{\infty}N^2(E)f(E)[1-f(E)]dE. \quad (6)$$

In Eqs. (2) and (6), $|\phi(0)|^2$ is the electronic probability amplitude at the resonant nucleus, normalized in an atomic volume Ω. The shift is proportional to the average $\langle|\phi(0)|^2\rangle$ of this quantity while the relaxation rate is proportional to its mean-square value $\langle|\phi(0)|^4\rangle$.

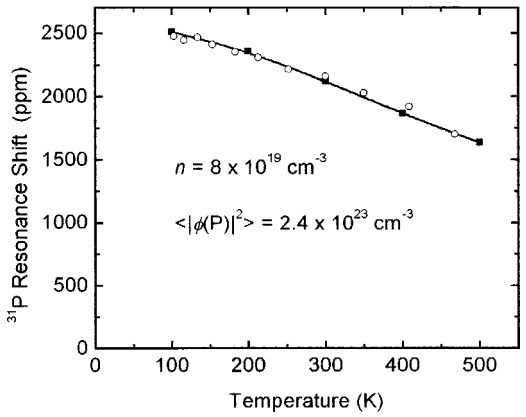

FIG. 8. Model calculation (closed points) based on Eq. (2) compared with experimental data (open points) for ^{31}P resonance shifts versus temperature for sample 80 ($n=8\times10^{19}$ cm^{-3}).

We have evaluated the integrals in Eqs. (2) and (6) to obtain the temperature dependence of the ^{31}P shift and relaxation rate at five temperatures over the range 100–500 K for $n=8\times10^{19}$ cm^{-3}. With the density of states given by Eq. (5), application of the condition of Eq. (4) shows that the chemical potential decreases from 63.0 to 37.8 meV over this temperature range. The results for $\Delta\nu/\nu$ and $1/T_1$ were scaled to the data using $\langle|\phi(P)|^2\rangle\Omega_P$ and $\langle|\phi(P)|^4\rangle\Omega_P^2$ as parameters. The calculations (Figs. 8 and 9) are in good agreement with the temperature dependence of the data, with the possible exception of the relaxation rate above 400 K. Because T/T_F is relatively small for this sample over the experimental temperature range, the results of these calculations also agree well with evaluation of the analytic expressions given by Hoch and Holcomb.[24]

Scaling the fits to the shifts and relaxation rates yielded $\langle|\phi(P)|^2\rangle\Omega_P=3010$ and $\langle|\phi(P)|^4\rangle^{1/2}\Omega_P=3760$, respectively. These results can be compared with the well-established value $|\phi(P)|^2=4.4\times10^{23}$ cm^{-3} obtained by electron spin

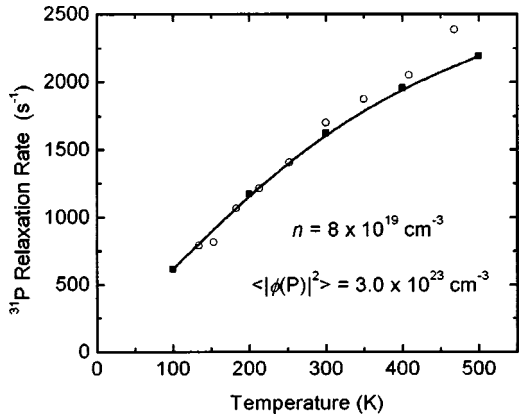

FIG. 9. Model calculation (closed points) based on Eq. (6) compared with experimental data (open points) for ^{31}P spin-lattice relaxation rates versus temperature for sample 80 ($n=8\times10^{19}$ cm^{-3}).

resonance[25] on the isolated impurity in dilute Si(P), i.e., $|\phi(P)|^2\Omega_P = 5500$ for $\Omega_P = 1/n = 1.25\times10^{-20}$ cm^3. The apparent reduction of $\langle|\phi(P)|^2\rangle\Omega_P$ by about 40% in the metal compared with the dilute impurity is reasonable. Together with the temperature dependence, this leads us to conclude that Eqs. (2) and (6) provide good quantitative representations of the data for our most heavily doped sample.

Scaling the ^{29}Si shift and relaxation data to those of ^{31}P in the range 250–300 K yields values $\langle|\phi(\mathrm{Si})|^2\rangle\Omega_{\mathrm{Si}} = 108$ and $\langle|\phi(\mathrm{Si})|^4\rangle^{1/2}\Omega_{\mathrm{Si}} = 125$, respectively. Because of slight differences in the temperature dependences of the ^{29}Si and ^{31}P data, these values can vary by 5–10 % depending on the range of data used. This variation may be related to the observed low temperature decrease of ^{29}Si signal intensity indicating that the distribution of silicon sites being sampled changes with temperature.

C. Impurity bands near the metal-nonmetal transition: $n = 4\times10^{18}$ cm^{-3}

The most lightly doped sample on which we obtained ^{31}P data (4) has a nominal phosphorous concentration very close to that of the metal-nonmetal transition ($n_{\mathrm{MNM}} = 3.8\times10^{18}$ cm^{-3}) observed at low temperatures.[2] This sample is highly nondegenerate at the temperatures of our experiments. If the donors were fully ionized with n electrons in the conduction band, the Fermi energy $\mu(0)$ would be 8.5 meV, i.e., $T_F = 99$ K. Assuming these conditions, one can evaluate the integrals of Eqs. (2) and (6) to predict the resonance shift and relaxation rate in the fully ionized limit. To do this, we have assumed that the quantities $\langle|\phi(P)|^2\rangle\Omega_P$ and $\langle|\phi(P)|^4\rangle^{1/2}\Omega_P$ retain the values given in the preceding section for the nearly degenerate sample (80). The results of this calculation are in poor agreement with the observations. The predicted ^{31}P shifts are much smaller than the observed values even though the temperature dependence is qualitatively similar. However, the predicted relaxation rates are not only much weaker than observed, but they tend to increase with temperature while the observed rates decrease strongly. Thus while the shift data might be reconciled with the "conduction band only" model by a relatively large adjustment of $\langle|\phi(P)|^2\rangle\Omega_P$, the relaxation data are qualitatively inconsistent with this approach. These failures of the "conduction band only" model as well as the sharply different NMR properties of ^{31}P and ^{29}Si motivated an alternative approach that takes into account electronic states specifically associated with the impurity.

The electronic states of the isolated P donor in Si have been studied extensively.[1] In the effective mass approximation, the impurity levels form a hydrogenic series consisting of a 1s ground state and excited states 2s, 2p, etc. These states are all sixfold degenerate because of the degeneracy of the conduction band minimum. However, corrections to the effective mass approximation lift some of the degeneracies of the impurity states. In particular, the 1s level splits into a nondegenerate ground state A_1, an excited doublet state (E), and an excited triplet (T_1). The higher-energy effective mass states are similarly split. Of particular importance for ^{31}P NMR properties is the fact that the A_1 ground state has local

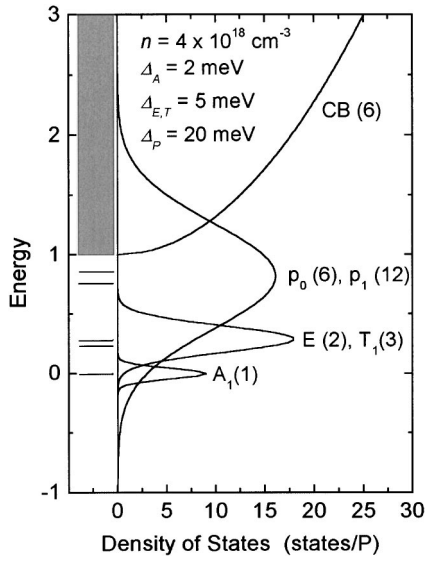

FIG. 10. Model density of states for sample 4 ($n = 4\times10^{18}$ cm^{-3}). Left-hand panel shows energy levels of isolated phosphorous donor in Si. Impurity bands with respective widths Δ_i are labeled with degeneracies in parentheses. Energy is expressed in units of the A_1 state binding energy (45 meV).

atomic s character, whereas the E and T_1 states as well as higher p_0 and p_1 states, are p like.[1] The hyperfine fields of electrons in impurity states should therefore be dominated by those in the A_1 ground state. The spectrum of low-lying states of the isolated donor are shown in the left-hand panel of Fig. 10.

To model the local electronic structure in the range of heavy doping, we assume that the sharp energy levels of the isolated impurity are broadened by impurity-impurity interactions to yield a series of Gaussian impurity bands of the general form

$$N_i(E) = g_i\sqrt{2/\pi\Delta_i^2}\,\exp[-(E-E_i)/2\Delta_i^2], \tag{7}$$

where E_i is the position of the band center derived from the ith impurity level, Δ_i is the band width and g_i is the degeneracy of the impurity state. For our model calculations, we consider four impurity bands at the following energies and degeneracies:

$$E_{A1} = 0, \quad g_{A1} = 1,$$

$$E_{E,T} = 11.7 \text{ meV}, \quad g_{E,T} = 5,$$

$$E_{\rho0} = 34.1 \text{ meV}, \quad g_{\rho0} = 6,$$

$$E_{p1} = 38.3 \text{ meV}, \quad g_{p1} = 12.$$

Because of their small energy separation, we assume that the E and T_1 states form a single fivefold degenerate impurity band. The conduction band minimum falls at $E_C = 45$ meV on this energy scale. These bands are illustrated in the right-hand panel of Fig. 10 with the parameters used for $n = 4\times10^{18}$ cm^{-3}.

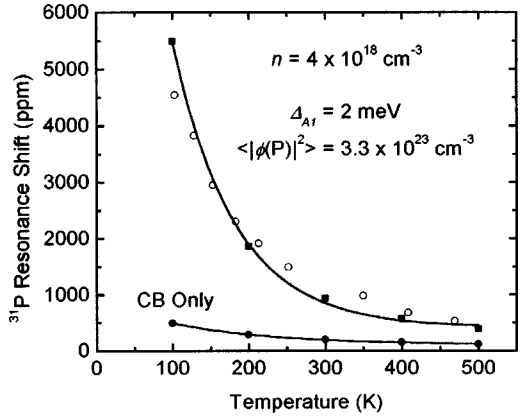

FIG. 11. Impurity band model calculations (solid squares) compared with experimental data (open circles) for ^{31}P resonance shifts for sample 4 ($n=4\times10^{18}$ cm^{-3}). Also shown (solid circles) are predicted results for complete impurity ionization ("CB only").

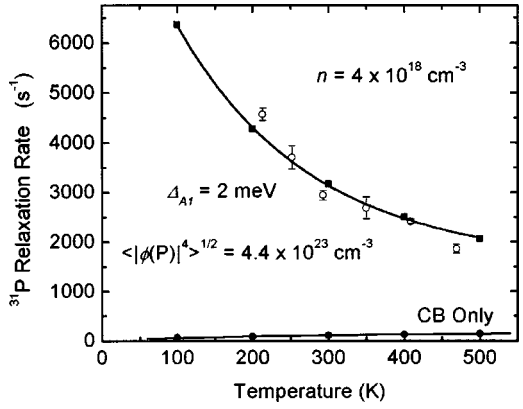

FIG. 12. Impurity band model calculations (solid squares) compared with experimental data (open circles) for ^{31}P spin-lattice relaxation rates for sample 4 ($n=4\times10^{18}$ cm^{-3}). Also shown (solid circles) are predicted results for complete impurity ionization ("CB only").

To determine the position of the chemical potential at each temperature, the total density of states used in Eq. (4) is

$$N_{\rm tot}(E) = \sum_i N_i(E) + N_{\rm CB}(E), \tag{8}$$

where $N_{\rm CB}(E)$ is given by Eq. (5). In this model, we assume that impurity states are progressively more severely broadened by impurity-impurity interactions and disorder with increasing energy. We neglect the effects of any states above the p_0,p_1 levels, assuming them to be merged with the conduction band states at this concentration.

For calculation of the NMR properties for $n=4\times10^{18}$ cm^{-3}, we assume that only the *s*-like A_1 states and the conduction states have significant hyperfine coupling to the ^{31}P nuclei. As we discuss in Sec. IV D, this condition is relaxed somewhat for modeling the higher dopant concentrations. For the conduction states $\langle|\phi(P)|^2\rangle\Omega_P$ and $\langle|\phi(P)|^4\rangle^{1/2}\Omega_P$ are assumed to have the same values as obtained for the most heavily doped sample (80). These quantities are taken to be fitting parameters for the A_1 band. The other free parameters are the impurity bandwidths Δ_i.

The results of our model calculations for $n=4\times10^{18}$ cm^{-3} are shown in Figs. 11 and 12. The bandwidths used for this calculation are $\Delta_{A_1}=2$ meV, $\Delta_{E,T}=5$ meV, and $\Delta_{p_0}=\Delta_{p_1}=20$ meV. In the fitting procedure, the bandwidths were adjusted to match the temperature dependence of the data, and the hyperfine couplings were fit to the overall scale. The hyperfine couplings for the A_1 band were taken to be $\langle|\phi(P)|^2\rangle=3.3\times10^{23}$ cm^{-3} for the shift and $\langle|\phi(P)|^4\rangle^{1/2}=4.4\times10^{23}$ cm^{-3} for the relaxation rate. The fits to the temperature dependence of $\Delta\nu/\nu$ and $1/T_1$ are not perfect, but this relatively simple model does reproduce the general features of the data with reasonable parameters. Also shown in Figs. 11 and 12 are the calculated results for the case of full ionization ("CB only") discussed above. The inadequacy of that approach is evident. It is likely that agreement with experiment could be improved by further elaboration of the model, but we doubt that such a solution would be unique. The main conclusion we wish to draw from these results is that inclusion of the effects of impurity bands provides an explanation of qualitative features of the data that deviate strongly from expectations for carriers confined to the conduction band. The model parameters provide estimates of average or effective impurity bandwidths for this concentration. In Sec. IV F we address the effects of disorder and the expectation that the impurity band structure varies from site to site within the samples.

The impurity band model leads to a picture of electronic transport in which carriers are in dynamic equilibrium between impurity and conduction band states. The effective mobility is therefore a weighted average of the mobilities of the various states occupied at a given temperature. The qualitative features of the Hall effect data for our samples are consistent with this idea, and with a substantially reduced mobility in the impurity bands. For nominal composition $n=4\times10^{18}$ cm^{-3}, for example, the apparent mobility at 77 K is about 40% of the room temperature value.

We have not attempted to model the Hall data with the same degree of detail as considered for the NMR properties. However, it is straightforward to show that the Hall results can be explained by a simple two-band model consisting of a conduction band and a single impurity band taken to represent the complex of impurity subbands discussed above. In such a case, the Hall coefficient at low magnetic fields can be written[26]

$$R = \frac{R_{\rm CB}\rho_{\rm IB}^2 + R_{\rm IB}\rho_{\rm CB}^2}{(\rho_{\rm CB}+\rho_{\rm IB})^2} \tag{9}$$

in which $R_{\rm CB}$ and $R_{\rm IB}$ are, respectively, the Hall coefficients associated with the conduction band and the impurity band, and $\rho_{\rm CB}$ and $\rho_{\rm IB}$ are the corresponding resistances. Introducing the respective carrier concentrations $n_i=|1/R_ie|$ and mobilities $\mu_i=1/ne\rho_i$, it is possible to express the apparent carrier concentration and mobility in the form

$$n_H = \left|\frac{1}{R_He}\right| = n\frac{[(g-1)f+1]^2}{(g^2-1)f+1}, \tag{10}$$

TABLE III. Fitting parameters for impurity band model.

Sample	Δ_{A_1} (meV)	f_{A_1}	$\Delta_{E,T}$ (meV)	$f_{E,T}$	Δ_{p_0,p_1} (meV)	f_{p_0,p_1}	Δ_Σ (meV)	f_Σ
4	2	1.00	5	0.0	20	0.0		
7	5	0.926	10	0.037	20	0.037		
10		0.0		0.0		0.0	20	0.18
80		0.0		0.0		0.0		0.0

$$\mu_H = \left| \frac{R_H}{\rho} \right| = \mu_{\mathrm{CB}} \left(\frac{n}{n_H} \right) \left(\frac{(g-1)f+1}{g} \right) \tag{11}$$

where $f \equiv n_{\mathrm{CB}}/n$ and $g \equiv \mu_{\mathrm{CB}}/\mu_{\mathrm{IB}}$.

As we show in the next section, the impurity band model calculations suggest that the fractional occupation of the conduction band is approximately $f=0.11$ for sample 4 at room temperature. In contrast, $f \ll 1$ at 77 K so that $n_H \sim n$ at this temperature. With this information, it is possible to solve Eq. (10) to obtain the mobility ratio $g \cong 5$. With the experimental value $\mu_H = 150$ cm^2/V s for the Hall mobility at 300 K, Eq. (11) then yields a value $\mu_{\mathrm{CB}} \cong 300$ cm^2/V s for the conduction band mobility in this sample. The impurity band mobility, $\mu_{\mathrm{CB}}/g \cong 60$ cm^2/V s is in agreement with the observed value $\mu_H = 61$ cm^2/V s and the expectation that impurity states dominate the transport properties at 77 K.

This two-band interpretation of the Hall data is oversimplified if, as assumed in our analysis of the NMR data, there are actually multiple impurity bands present at this composition. For example, some of the carriers attributed to the conduction band in the analysis of the Hall coefficient, might actually occupy states in the upper impurity bands. Moreover, as pointed out by Holcomb,[27] the relation $n_{\mathrm{IB}} = |1/R_{\mathrm{IB}}e|$ may be subject to a correction factor for samples near MNM transition. Nevertheless, the two-band model is sufficient to show that the general features of the Hall data can be understood in terms of impurity states of substantially lower mobility than the conduction band states and which are depleted by thermal excitation with increasing temperature. The overall picture is consistent with our conclusions from the NMR data.

D. Intermediate concentrations (4×10^{18} cm^{-3} $< n \leqslant 1\times10^{19}$ cm^{-3})

The foregoing discussion shows that the magnitudes and temperature dependences of the ^{31}P resonance shifts and relaxation rates can be explained for the limiting cases of our most heavily and most lightly doped samples. For sample 80, it is sufficient to use a conventional metallic model with a density of states corresponding to free electrons with the conduction electron effective mass. In contrast, for sample 4 at the lower limit of the "transition range," the conduction band alone cannot account for the results. We have invoked an impurity band model in which the shift and relaxation rate are dominated by hyperfine interactions with electrons in the lowest *s*-like (A_1) band.

The shift and relaxation data for samples 7 and 10 indicate that impurity band effects remain important at these concentrations, albeit in modified form. For example, the relaxation rate for sample 7, similar to that of sample 4, increases with decreasing temperature. The rate for sample 10 is nearly independent of temperature with a weak maximum in the range investigated. In contrast, our numerical calculations using the "conduction band only" model predict a 50% increase in the relaxation rate between 200 and 400 K. Simply adjusting the hyperfine coupling strength $\langle|\phi(P)|^4\rangle^{1/2}\Omega_P$ is insufficient to reconcile this model with the experiment.

For these intermediate concentrations we assume the existence of an impurity band structure that is modified in two ways by the effects of increased disorder and mutual interactions among impurity states. First, we assume that the average impurity bandwidths increase due to increased impurity-impurity overlap at higher concentrations. Second, we assume that disorder tends to destroy the "pure" *s*- and *p*-like symmetries of the lowest and the excited state bands, respectively. These effects are parametrized by the bandwidths Δ_i and fractional weightings f_i of the hyperfine fields for the various impurity bands. For sample 10, we assumed that the impurity bands have collapsed into a single band Σ centered at the degeneracy-weighted average energy of the individual impurity bands considered. Because of the number of model parameters available, we do not believe that detailed fits to the data for the intermediate samples would be justified—the resulting fitting parameters are unlikely to be unique. Rather, we have chosen to search for parameter sets that reproduce the qualitative features of the experimental data and provide a reasonable picture of the evolution of the electronic structure from the low concentration limit to the "conduction band only" metallic limit. These parameters are presented in Table III. The corresponding simulations of the temperature dependent ^{31}P resonance shifts and relaxation rates are presented in Figs. 13 and 14, respectively.

Comparison of Figs. 13 and 14 with Figs. 3 and 4 shows that the impurity band model yields a semiquantitative account of the features of the evolving shift and relaxation behavior with increasing dopant concentration. We are, in fact, unable to account for the magnitudes and temperature dependences of the ^{31}P shifts and relaxation rates for $n \leqslant 1 \times 10^{19}$ cm^{-3} without assuming an important role for the impurity states. The dramatic qualitative differences in the NMR properties, especially the ^{31}P relaxation rates, reflect progressive destruction of the impurity band structure with increasing concentration. This evolution is illustrated in Fig. 15 for the *s* part of the impurity bands using the parameters given in Table II. The general features of this progression are reminiscent of the results calculated by Serre and Ghazali using a multiple-scattering approach.[28]

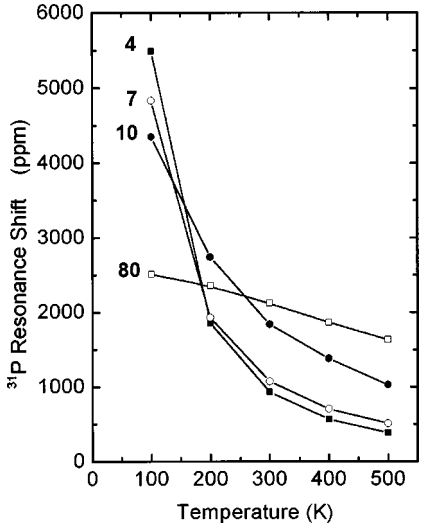

FIG. 13. Simulated ^{31}P resonance shifts versus temperature for all samples. Compositions are indicated in units of 10^{18} cm^{-3}.

The higher energy non-*s*-impurity bands (not shown in Fig. 15) play an important role in this model even though their direct contributions to the ^{31}P shifts and relaxation rates are small. The main influence of these bands is to determine the position of the chemical potential which, at the temperatures of our experiments, is always well below the energy of the A_1 band. For samples in the "transition range" (4—10 $\times 10^{18}$ cm^{-3}), therefore, occupation of the conduction band remains relatively low. This is illustrated in Fig. 16 which shows the fractional occupation of the conduction band predicted by our model as a function of temperature for the three compositions in the transition range.

E. Spin susceptibility

Although the paramagnetic spin susceptibility was not the primary focus of these experiments and the subsequent modeling, it is interesting to compare the predictions of the impurity band model with experimental data for the spin susceptibility. For this purpose, we use the absolute spin susceptibility values obtained by Quirt and Marko[5] from calibrated measurements of the electron spin resonance (ESR) intensity at 77 K. We compare our results for the two limiting cases for which we have carried out the most detailed fits to the impurity band model, our samples "4" and "80." We consider separately the *s*-electron component of the susceptibility, i.e., that part relevant for ^{31}P NMR properties, and the total spin susceptibility including contributions from the "NMR invisible" *p*-type impurity bands. We have also

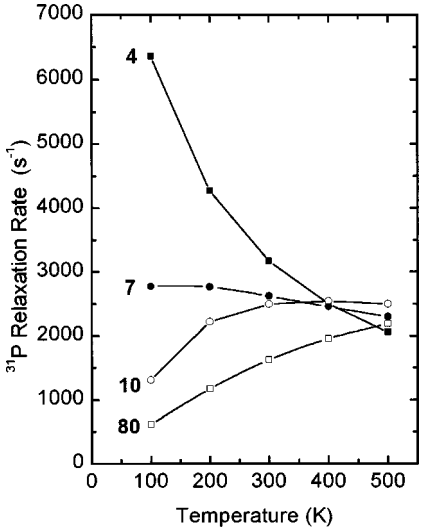

FIG. 14. Simulated ^{31}P spin-lattice relaxation rates versus temperature for all samples. Compositions are indicated in units of 10^{18} cm^{-3}.

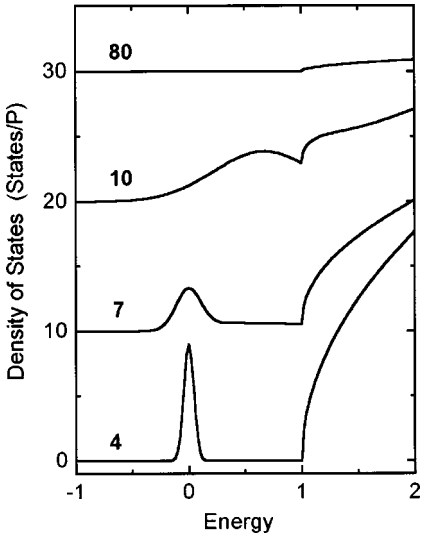

FIG. 15. Model density of states per phosphorous impurity (*s* part only) used for simulations shown in Figs. 13 and 14. The *p* bands shown in Fig. 10 are omitted, and the curves for samples 7, 10, and 80 are offset by 10, 20, and 30 states/P for clarity. Energy unit is the A_1 state binding energy (45 meV).

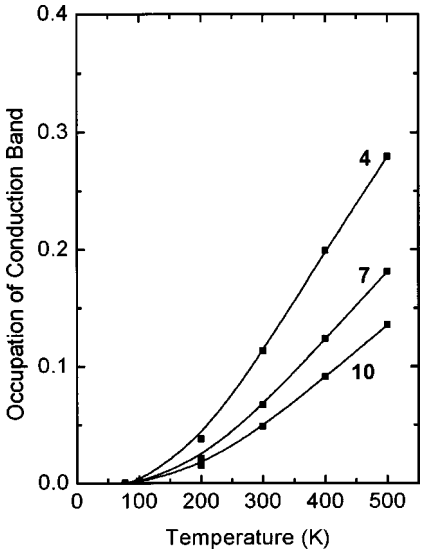

FIG. 16. Fractional occupation of conduction band versus temperature predicted by impurity band model for "transition range" samples of varying nominal concentration (in 10^{18} cm^{-3}).

TABLE IV. Paramagnetic spin susceptibility values at 77 K in 10^{-8} emu/g calculated for samples 4 and 80 compared with experimental values of Quirt and Marko (Ref. 5).

Sample	$\chi_{IB(s)}$ (calc)	$\chi_{IB(tot)}$ (calc)	χ_{CB} (calc)	χ (expt)
4	0.75	1.43	1.00	0.86
80			4.4	3.7

calculated, for comparison, the predicted susceptibility from the "conduction band only" model. These results are summarized in Table IV.

For sample 4, the calculated values in Table IV "bracket" the experimental value, i.e., consideration of the *s* bands alone underestimates χ while inclusion of contributions from the *p* bands leads to an overestimate. This comparison shows, nevertheless, that the model yields values for the spin susceptibility that are in the right range. It is not clear whether the discrepancies reflect only deficiencies in the model or also, perhaps, reduced ESR sensitivity to electrons in the more severely broadened *p* bands.

Despite the potential complication of the *p* bands, we might expect to see a convergence of the NMR shift and spin susceptibility at temperatures sufficiently low that both are dominated by electrons in the *s*-like A_1 ground state. This is borne out by the data shown in Fig. 17 in which the ^{31}P resonance shift is compared with the relative temperature dependence of the ESR intensity measured[29] on our samples 4 and 7. This plot shows that the temperature dependence of the shift, extrapolated below 100 K is consistent with the temperature dependence of the ESR intensity.

F. Effects of disorder: Inhomogeneous broadening

A doped semiconductor is inherently disordered by the random distribution of impurity atoms on host lattice sites.

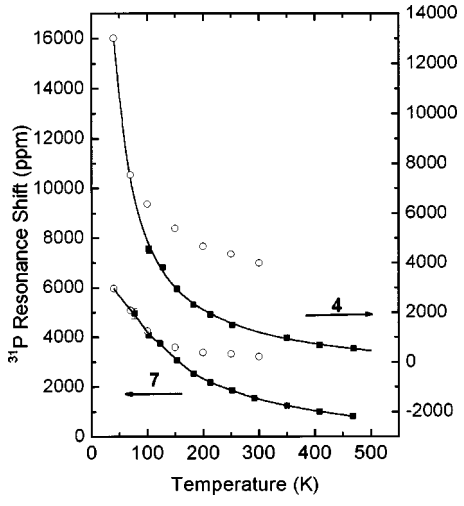

FIG. 17. Comparison of the temperature dependence of the ^{31}P resonance shifts for samples 4 and 7 (solid points) with that of the ESR intensity (open points). ESR intensity in arbitrary units is scaled to the resonance shift. Right-hand scale (sample 4) is offset for clarity.

The consequences of disorder in Si:P are quite evident in the low temperature ^{31}P NMR results of Alloul and Dellouve.[10] As discussed above, those experiments yielded extremely broad spin-echo spectra, typically an order of magnitude broader than observed in the present work. The spin-lattice relaxation rates varied with frequency within these spectral lines and were in general agreement with the Korringa relation for the shift associated with the measurement frequency. The observed ^{31}P nuclei were therefore in essentially metallic environments. The strongly temperature-dependent magnetic susceptibility observed in their samples was attributed to local moments on relatively isolated P impurities on which strong, slowly fluctuating hyperfine fields broadened the NMR line to invisibility.

The general characteristics observed by Alloul and Dellouve contrast sharply with those of the present experiment. At temperatures above about 100 K, the spin-echo spectra are essentially homogeneous as is illustrated, for example, by the data in Fig. 1. The linewidth data shown in Fig. 2 suggest the presence of two components: a temperature-independent component that increases with the concentration of impurities and a component that increases at lower temperatures. The onset of temperature-dependent broadening is particularly striking in samples 7 and 10. This effect tends to occur at a lower temperature in the samples of lower phosphorous concentration. The exception to this pattern is the most heavily doped sample, 80, for which broadening exceeds the change of shift at all temperatures and a temperature-independent component is not discernable.

Sundfors and Holcomb[3] and Holcomb[30] have suggested a broadening mechanism that is essentially structural, related to the random distribution of phosphorous donors of which some carry local magnetic moments at low temperatures. In the more dilute samples, significant numbers of ^{31}P nuclei are well separated from other donors and experience relatively homogeneous local environments. As the concentration increases, disorder in the local environments increases accordingly. Sundfors and Holcomb[3] developed a model of ^{31}P broadening along these lines based on a Poisson distribution for the number of phosphorous atoms within a certain critical volume.

Broadening due to the local moments must certainly be present and important at sufficiently low temperatures. It is unclear the extent to which this broadening mechanism is effective in the temperature range of our experiments. However, the impurity band model provides an alternative explanation of the temperature-dependent broadening, and the apparent contradiction between the high- and low-temperature ^{31}P NMR spectra. The impurity bandwidths are primarily determined by impurity-impurity interaction effects so that we can expect the bandwidths to vary within the sample according to the local concentration of P impurities. To the extent that k_BT is small compared with the impurity bandwidths, the resonance shift and relaxation rates can be expected to be very sensitive to the local bandwidth and density of states associated with the local impurity level, i.e., the A_1 states. This condition certainly applies at 4.2 K and below where k_BT (0.4 meV at 4.2 K) is much smaller than the bandwidths of several meV inferred from the data at 100 K and higher. In contrast, the convolution of the Fermi function

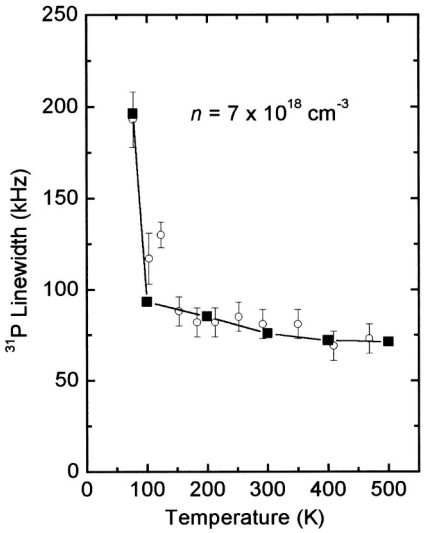

FIG. 18. ^{31}P linewidth (open points) versus temperature for sample 7 ($n=7\times10^{18}$ cm^{-3}) compared with the sensitivity of the calculated shift (solid points) to the width of the A_1 impurity band when the latter is increased from 5 to 10 meV. The derivative $d(\Delta\nu)/d(\Delta_{A_1})$ thus estimated has been scaled to the data and a constant was added to account for the temperature-independent component of the linewidth.

with the impurity band density of states of Eqs. (2) and (6) becomes increasingly insensitive to the impurity bandwidth when k_BT exceeds that bandwidth. In this limit, the impurity bandwidths inferred from the model calculations should be viewed as averages for a given sample composition.

We have examined the sensitivity of the shift to the impurity bandwidth by calculating the change of shift predicted by the model for sample 7 when the width of the A_1 band is doubled from 5 to 10 meV. This rough estimate of the derivative $d(\Delta\nu)/d(\Delta_{A_1})$, scaled to the linewidth data, is plotted against temperature in Fig. 18. A constant has been added to account for the temperature-independent linewidth component. This procedure yields a reasonable representation of the gradual increase in linewidth observed above about 150 K and, in agreement with experiment, shows a sharp onset of additional broadening below 100 K as k_BT becomes comparable with the impurity bandwidth.

This approach provides an explanation for the temperature dependent broadening observed for samples 7 and 10, and the absence of a broadening onset in the temperature range studied for sample 4 for which our model suggests a narrower A_1 band. The success of this comparison also provides an independent indication that our inferred impurity bandwidths of a few meV are of the correct magnitude. As noted above, however, the present description of the broadening onset is incomplete since the possible effects of local moment formation are not considered. Furthermore, since all the available information indicate that the impurity bands are absent in the very heavily doped sample 80, the broadening observed for that sample must have another origin.

G. ^{29}Si interpretation

The foregoing interpretive discussion has emphasized the experimental results for ^{31}P and their implications for the local impurity electronic structure. We have not attempted a detailed interpretation of the ^{29}Si results. Nevertheless, we conclude this discussion with some general remarks about the ^{29}Si NMR properties. The first point is to recognize the inherent inhomogeneity of the ^{29}Si environments. It is clear from the concentration dependences evident in the data in Figs. 5–7 that the ^{29}Si environments are profoundly affected by the presence of the donors in the material. However, some of the ^{29}Si are as close as nearest neighbors to the donors while others are some distance away. Even if the donors were ordered on a periodic superlattice so that the ^{31}P environments were identical, the ^{29}Si NMR data would still represent a superposition of results from various sites. It is quite possible, in fact, that the ^{29}Si very close to the donors do not contribute to the observed signal as a result of strong shifts and rapid relaxation on those sites. The observation in our experiments that ^{29}Si intensity decreased with decreasing temperature is consistent with this expectation.

To the extent that the ^{29}Si line is weighted by sites more distant from the donor, we should expect that conduction states are relatively more influential than are the impurity states. There is a hint of this in the ^{29}Si relaxation data (Fig. 7) which exhibit a temperature dependence that is qualitatively similar to that of the conduction band occupation shown in Fig. 16. The corresponding resonance shifts (Fig. 5), however, do not exhibit the same tendencies. The loss of signal intensity means that the apparent temperature dependences of the resonance shifts and relaxation rates do not reflect the temperature-dependent environments of a fixed subset of the ^{29}Si sites. It is possible, for example, that some of the more rapidly relaxing sites begin to contribute to the observed resonances at higher temperatures leading to the upward curvature of the $1/T_1$ plots of Fig. 7. Without a better understanding of the intensity loss, we believe that it is difficult to justify an attempt at detailed interpretation of these data.

For purposes of the present study, the importance of the ^{29}Si results is their qualitative difference from those of the ^{31}P impurity. These differences persist even in the higher-temperature ranges in which the ^{29}Si intensity remains constant. It is apparent that the host and impurity nuclei are coupling to different subsets of extrinsic electrons. This is *prima facie* evidence for a local electronic structure at the donor that is distinct from that associated with extended conduction band states.

V. SUMMARY

We have described a comprehensive study of the ^{31}P and ^{29}Si NMR properties of nominally metallic Si:P samples over a range of temperatures from approximately 100 K to nearly 500 K. Except for the most heavily doped sample, the ^{31}P results exhibit a variety of complex behaviors that are inconsistent with the picture conventionally applied to Si:P at these relatively high temperature conditions, namely that of fully ionized donors and carriers confined to extended conduction band states. Two features of the results are particularly persuasive with respect to this observation. One is the qualitative difference between the temperature dependences

of the resonance shifts and relaxation rates of the host and impurity nuclei. While both species are strongly affected by their hyperfine interactions with extrinsic electrons, the data imply that the ^{29}Si and ^{31}P nuclei couple predominantly to electrons in distinctly different sets of states. The second feature is the observation of temperature dependences for the ^{31}P spin-lattice relaxation rates for samples with nominal concentrations in the range 4×10^{18} to 1×10^{19} cm^{-3} that are qualitatively inconsistent with expectation for free carriers in a conduction band. In the case of samples with concentrations 4×10^{18} and 7×10^{18} cm^{-3}, even the *sign* of the temperature dependence is opposite to the prediction of the conventional model.

In light of these failures of a "conduction band only" model, we have assumed that a complex of impurity bands survives in some form to doping levels as high as 10^{19} cm^{-3}. To demonstrate the plausibility of this assumption, we developed a numerical model and simulated the relaxation rate and resonance shift results for the samples studied. The model bands are interpreted as representing the average effect of impurity bands whose actual widths vary from site to site as a result of the inherent disorder in the doped semiconductor. This averaging is effective at temperatures for which k_BT exceeds the typical local impurity bandwidths. Violation of this condition explains, at least in part, the striking contrast between the relatively homogeneous NMR behavior observed above 100 K and the highly inhomogeneous distribution of local electronic character evident in ^{31}P data obtained at 4.2 K and below. The rapid onset of additional line broadening in some samples is attributed to breakdown of the high-temperature condition with decreasing temperature.

The model computations provide a semiquantitative simulation of the high-temperature ^{31}P data. The dominant effect influencing the temperature dependence of the relaxation rates and shifts is thermal depletion of the lowest impurity levels which have *s*-like local symmetry at the ^{31}P nuclei. The presence of higher energy, *p*-like impurity states is profoundly important in establishing the chemical potential and conduction band occupation at a given temperature even though these states do not contribute directly to the ^{31}P hyperfine properties. The model parameters provide estimates of the average impurity bandwidths and a qualitative picture of the evolution of the impurity band complex with increasing phosphorous concentration in the so-called "transition range" between the MNM transition and 1×10^{19} cm^{-3}. Data obtained in the very heavily doped sample (8×10^{19} cm^{-3}) are explicable in terms of electrons exclusively occupying conduction band states—there is no evidence of residual impurity band effects at this composition.

These results have implications for a picture of electronic transport in heavily doped silicon at room temperature and above. The qualitative features of the ^{31}P data that we attribute to occupied impurity bands persist to the highest temperatures investigated, approximately 470 K. A significant fraction of the extrinsic electrons (a majority according to our model) occupy impurity band states even at these high temperatures and should be in dynamic equilibrium with conduction states. This implies that values of transport properties such as the dc conductivity or the Hall coefficient measured at room temperature reflect averages of impurity and conduction band characteristics. The temperature dependences of the Hall coefficient and apparent carrier concentrations measured in our samples and by others are consistent with this multiband picture of Si:P in the "transition range" of dopant concentration.

ACKNOWLEDGMENTS

In the course of digesting and interpreting the results of these experiments, the authors maintained extended correspondence with D. F. Holcomb and M. J. R. Hoch. We have benefited greatly from their years of experience and critical thinking about the electronic properties of doped silicon, their willingness to share their ideas in the form of numerous stimulating suggestions, and from several highly relevant references that they brought to our attention. The heavily doped sample (80) was provided to us by Professor Holcomb. For all this, we are deeply appreciative. We also wish to express our thanks to J. Tate who put her Hall measurement apparatus at our disposal, to M. Price who assisted with the Hall measurements, and to B. Meier, A. Hofstaetter, and D. M. Hofmann for electron spin-resonance measurements. We are grateful to H. Alloul, T. G. Castner, H. Jansen, and T. M. Rice who contributed to this work with helpful discussions of the impurity band problem. This work was supported in part by National Science Foundation Grants No. DMR-9623299 and DMR-0071898.

*Present address: MRC/UCT Medical Imaging Research Unit, Department of Human Biology, Faculty of Health Sciences, University of Cape Town, Observatory 7925, South Africa.

[1] See, for example, W. Kohn in *Solid State Physics*, edited by F. Seitz and D. Turnbull (Academic, New York, 1957), Vol. 5, p. 257.

[2] T. F. Rosenbaum, K. Andres, and G. A. Thomas, Solid State Commun. **35**, 663 (1980); T. F. Rosenbaum *et al.*, Phys. Rev. B **27**, 7509 (1983).

[3] R. K. Sundfors and D. F. Holcomb, Phys. Rev. **136**, A810 (1964).

[4] H. Ue and S. Maekawa, Phys. Rev. B **3**, 4232 (1971).

[5] J. D. Quirt and J. R. Marko, Phys. Rev. Lett. **26**, 318 (1971); Phys. Rev. B **7**, 3842 (1973).

[6] G. C. Brown and D. F. Holcomb, Phys. Rev. B **10**, 3394 (1974).

[7] W. Sasaki, S. Ikehata, and S. Kobayashi, J. Phys. Soc. Jpn. **36**, 1377 (1974).

[8] S. Ikehata, W. Sasaki, and S. Kobayashi, J. Phys. Soc. Jpn. **39**, 1492 (1975).

[9] S. Kobayashi, Y. Fukagawa, S. Kiehata, and W. Sasaki, J. Phys. Soc. Jpn. **45**, 1276 (1978).

[10] H. Alloul and P. Dellouve, Phys. Rev. Lett. **59**, 578 (1987); J. Phys. (France) **49**, 1185 (1988).

[11] M. J. R. Hoch and D. F. Holcomb, Phys. Rev. B **38**, 10 550 (1988).
[12] M. J. Hirsch, D. F. Holcomb, R. N. Bhatt, and M. A. Paalanen, Phys. Rev. Lett. **68**, 1418 (1992).
[13] A. Gaymann, H. P. Geserich, and H. v. Lohneysen, Phys. Rev. B **52**, 16 486 (1995).
[14] For a review of much of the earlier NMR work, see D. F. Holcomb, in *Proceedings of the 31st Scottish Universities Summer School in Physics*, edited by D. M. Finlayson (University of Edinburgh Press, Edinburgh, 1986).
[15] S. E. Fuller, E. M. Meintjes, and W. W. Warren, Jr., Phys. Rev. Lett. **76**, 2806 (1996).
[16] Virginia Semiconductor, Fredericksburg, VA.
[17] The Hall effect measurements form the basis of a Senior Thesis in Physics at Oregon State University by Jeremy Danielson.
[18] It has been suggested that the apparent power law behavior for the ^{29}Si relaxation rates might be better represented by variable range hopping behavior whereby $1/T_1 \propto \exp[-(t_0/T)^{1/2}]$. We checked this by plotting the relaxation rates for samples 2, 4, 7, and 10 in the form $\ln(1/T_1)$ versus $(1/T)^{1/2}$. The fit was found to be inferior to the power law fits. We emphasize, nevertheless, that the power law fits are merely empirical representations of the observed temperature dependence. We have proposed no physical mechanism for this behavior.
[19] I. Granächer and W. Czaja, J. Phys. Chem. Solids **28**, 231 (1967).
[20] C. Yamanouchi *et al.*, J. Phys. Soc. Jpn. **22**, 859 (1967).
[21] Our interpretation of the ^{31}P NMR results does not include the possible influence of exchange effects on the susceptibilities responsible for the shifts and relaxation. We cannot exclude a role for such effects. However, as we show below, the observations can be explained in the context of a model based on noninteracting electrons.
[22] J. Korringa, Physica (Amsterdam) **16**, 601 (1950).
[23] N. W. Ashcroft and N. D. Mermin, *Solid State Physics* (Saunders, Philadelphia, 1976), p. 45.
[24] M. J. R. Hoch and D. F. Holcomb, following paper, Phys. Rev. B **71**, 035115 (2005).
[25] R. C. Fletcher, W. A. Yager, G. L. Pearson, and F. R. Merritt, Phys. Rev. **95**, 844 (1954).
[26] N. W. Ashcroft and N. D. Mermin, *Solid State Physics* (Saunders, Philadelphia, 1976), p. 240.
[27] D. F. Holcomb (private communication) has pointed out that for samples near the MNM transition, the carrier concentration is more accurately expressed as $n=|A/R_H e|$, where the constant A may be as high as $A \cong 1.3$ [P. F. Newman, M. J. Hirsch, and D. F. Holcomb, J. Appl. Phys. **58**, 3779 (1985)]. We have tested the two-band analysis of the Hall data assigning $A=1.3$ to the impurity band and $A=1.0$ to the conduction band. The effect of this refinement is to reduce the calculated value of the mobility ratio from $g \cong 5$ for $A=1$ to $g \cong 4.4$ for $A=1.3$. The corresponding mobility values are $\mu_{CB}=275$ cm^2/V s and $\mu_{IB}=63$ cm^2/V s for $A=1.3$ compared with 300 cm^2/V s and 60 cm^2/V s, respectively, for $A=1$. In the context of the simple models being used for this analysis, we do not consider these differences to be significant.
[28] J. Serre and A. Ghazali, Phys. Rev. B **28**, 4704 (1983).
[29] Electron spin resonance characterization of our samples was carried out by A. Hofstaetter in the laboratory of B. K. Meyer at the Universität Gießen, Germany.
[30] D. F. Holcomb (private communication).